Published in final edited form as:
Nat Cell Biol. 2009 July ; 11(7): 807–814. doi:10.1038/ncb1887.

SDPR induces membrane curvature and functions in the formation of caveolae

Carsten G. Hansen[1], **Nicholas A. Bright**[2], **Gillian Howard**[1], and **Benjamin J. Nichols**[1]
[1]MRC-LMB, Hills Road, Cambridge, CB2 0QH, UK

[2]University of Cambridge, Cambridge Institute for Medical Research, Addenbrooke's Hospital, Hills Road, Cambridge, CB2 0XY, UK

Abstract

Caveolae are plasma membrane invaginations with a characteristic flask shaped morphology. They function in diverse cellular processes, including endocytosis. The mechanism by which caveolae are generated is not fully understood, but both caveolin proteins and Polymerase I and Transcript Release Factor (PTRF, also called cavin) are important. Here we show that loss of SDPR, a caveolar protein homologous to PTRF, causes loss of caveolae. SDPR binds directly to PTRF and recruits PTRF to caveolar membranes. Over-expression of SDPR, unlike PTRF, induces deformation of caveolae and extensive tubulation of the plasma membrane. The B-subunit of shiga toxin (STB) also induces membrane tubulation, and these membrane tubes also originate from caveolae. STB co-localizes extensively with both SDPR and caveolin 1. Loss of caveolae reduces the propensity of STB to induce membrane tubulation. We conclude that SDPR is a membrane-curvature inducing component of caveolae, and that STB-induced membrane tubulation is facilitated by caveolae.

Introduction

Various endocytic pathways operate in mammalian cells. The number, mechanism and specific functions of these pathways are currently under investigation 1. Three paradigms inform current models for how endocytic vesicles are generated; reversible association of cytosolic coat proteins leads to formation of clathrin-coated pits 2, 3, stable membrane association of caveolin proteins leads to formation of morphologically stable caveolae and caveolar vesicles 4-9, and tubulation of the plasma membrane can result in endocytosis in processes that are not well defined in molecular terms 1, 10, 11. Recently it was shown that extracellular ligands such as the glycosphingolipid binding B-subunit of shiga toxin (STB) induce their own endocytosis in tubular membrane invaginations 12-14. Several important questions remain to be addressed. Biogenesis of caveolae requires both caveolin and PTRF (cavin) proteins 15-20, but the identity, function and molecular interactions of further caveolar components remain unresolved. STB induces formation of membrane tubes even in ATP-depleted cells 12, but whether such tubes arise solely from interaction of the toxin with membrane lipids or require additional membrane or cytosolic proteins remains unclear. Here we provide new data to address both of these questions. We show that loss of SDPR, a caveolar protein homologous to PTRF 21-23, causes loss of caveolae. SDPR binds directly to PTRF and recruits PTRF to caveolar membranes. Over-expression of SDPR, unlike PTRF, induces deformation of caveolae and extensive tubulation of the plasma membrane. SDPR-induced tubes originate from caveolae, and incorporate STB. The membrane tubes induced by STB also originate from caveolae, and STB co-localizes extensively with both

Correspondence should be addressed to BJN, ben@mrc-lmb.cam.ac.uk, tel. +44 1223 402229, fax + 44 1223 412142.

Europe PMC Funders Author Manuscripts

Europe PMC Funders Author Manuscripts

SDPR and caveolin 1. Loss of SDPR, PTRF or caveolin 1 reduces the propensity of STB to induce membrane tubulation. We conclude that SDPR is a membrane curvature inducing component of caveolae, and that the tubes induced by STB in cells reflect interaction of toxin-glycosphingolipid complexes with caveolar proteins.

Results and Discussion

PTRF, Polymerase I Transcript Release Factor (also termed cavin), is a caveolar protein, and is required for formation of characteristic omega-shaped caveolar membrane invaginations 15-18, 20. There are three proteins in the human genome with a primary structure >20% identical to PTRF (Supplementary Figure 1, and http://www.treefam.org, accession TF331031). They are SDPR (serum deprivation protein response 22-24), SRBC (sdr-related gene product that binds to c-kinase, also called PRKCDBP 22, 25) and MURC (muscle restricted coiled coil protein 26, 27). SDPR co-localizes with caveolin 1 23, 25. We constructed plasmids for expressing fluorescent chimeras of PTRF, SDPR, SRBC and MURC in mammalian cells. All four chimeras co-localized well with caveolin 1 in HeLa cells, and are thus likely to be recruited to caveolae (Supplementary Figure 2). This study focuses on SDPR, because of its ability to induce membrane tubulation as detailed below.

SDPR is required for stable expression of PTRF and caveolin 1

A polyclonal antibody against peptides corresponding to amino acids 9-23 and 312-325 of human SDPR was raised in rabbits. After affinity purification, the SDPR antibodies recognized a band of 49kDa on Western blots of HeLa cell extracts. This corresponds to the predicted molecular mass of SDPR. A higher molecular weight band was also observed (Figure 1A). Two HeLa cell lines stably transfected with plasmids expressing short hairpin RNAs (shRNAs) specific to different regions of the SDPR mRNA were generated. In both SDPR shRNA cell lines the 49kDa band was reduced to less than 15% of the levels observed in control cells (cells stably transfected with empty shRNA vector used or non-targeting shRNA - only the latter is shown). The SDPR shRNA cell lines therefore provide a good system to investigate SDPR function. Cell lines expressing shRNAs against PTRF were also generated (Figure 1A).

Western blotting of control, SDPR shRNA and PTRF shRNA cell lines showed that reduction in SDPR expression causes loss of PTRF protein, and *vice versa* (Figure 1A). Reduction in either PTRF or SDPR expression also caused a loss of caveolin 1 expression. SDPR shRNA cell lines were transiently transfected with a plasmid expressing SDPR-CFP with silent mutations to the nucleotides recognized by the shRNA. Protein expression levels in transfected and non-transfected cells were compared after FACS sorting. Expression of the non-targeted SDPR-CFP was sufficient to rescue the expression of PTRF and caveolin 1 (Supplementary Figure 3A), confirming that loss of PTRF and caveolin 1 expression in these cells is due to reduced expression of SDPR, and thereby implying that SDPR, PTRF and caveolin 1 are functionally interdependent.

Indirect immunofluorescence labeling of HeLa cells with the SDPR antibody revealed a high degree of co-localization with caveolin 1 in some cells (Figure 1B), but in others non-specific background labeling (as judged by labeling of SDPR shRNA cell lines) was apparent, presumably because SDPR expression was lower in these cells. Labeling of both transfected and neighboring untransfected cells with the antibody allowed us to obtain an estimate of the minimum fold over-expression of SDPR-mCherry (Supplementary Figure 3B). Expression of SDPR-mCherry (mCh) at low levels (less than 3x endogenous) resulted in a high degree of co-localization with caveolin 1. Use of Total Internal Reflection (TIR) microscopy to illuminate the bottom 100nm of the cell 28 confirmed that over 80% of plasma membrane puncta containing caveolin 1 also contain SDPR-mCh (Figure 1C). When

over-expressed more than 5-fold, SDPR was observed in profuse membrane tubes as well as puncta (Figure 1D). SDPR-GFP behaved in the same way as SDPR-mCh. When PTRF-mCh was expressed at the same levels it accumulated in the cytosol, (Figure 1D).

PTRF and SDPR bind to each other, and form complexes also containing caveolin 1

The findings that SDPR, like PTRF 15-18, colocalizes with caveolin 1, and that when expression of either SDPR or PTRF is reduced the expression of the other two members of this trio also goes down, suggested that SDPR, PTRF and caveolin 1 might be present in the same complex. Our antibodies did not efficiently precipitate endogenous SDPR, so immunoprecipitation of either PTRF-GFP or SDPR-GFP from cell lysates prepared by solublization in 1% n-β-Octylglycoside and 1% Triton X-100 with anti-GFP antibodies was carried out. In both cases this resulted in specific co-precipitation of epitope tagged SDPR (Figure 2A). Immunoprecipitation of SDPR-GFP also resulted in specific co-precipitation of endogenous PTRF and caveolin 1 (Figure 2B). The simplest explanation for these results is the presence of a protein complex containing all three proteins.

We used bacterially expressed and purified PTRF and SDPR to test whether these proteins bind to each other. Full length PTRF was degraded within the bacterial cells, but we found that a construct containing the conserved coiled-coil and basic regions (6His-PTRF47-268) could be isolated intact. Full length GST-SDPR was also slightly degraded, albeit less than 6His-PTRF, as was GST-SDPR49-274 (SDPR49-274 comprises the minimal region of the protein required for membrane targeting and tubulation, as shown below). 6His-PTRF47-268 clearly bound highly efficiently and specifically to both GST-SDPR and GST-SDPR49-274 (Figure 2C). In order to double-check that the Coomassie-stained band corresponding in size to 6His-PTRF47-268 eluted bound to the SDPR constructs really is PTRF we used western blotting with anti-PTRF antibodies (Figure 2C). PTRF and SDPR therefore do indeed bind to each other directly and specifically, and this interaction does not require the presence of caveolin 1.

SDPR plays a direct role in biogenesis of caveolae

PTRF is required for production of normal levels of caveolae 15, 16, 20. As reduction in SDPR expression causes concomitant reductions in the expression of PTRF and caveolin 1, one would expect to see the same phenotype in the SDPR shRNA cell lines. We counted the number of plasma membrane caveolae in electron micrographs representing complete sections (Supplementary Figure 4) through cells from control and SDPR shRNA cell lines, and observed the predicted loss of caveolae (Figure 3A).

It was possible that the role of SDPR is limited to stabilizing PTRF and caveolin 1 expression. In order to address this we first compared the number of caveolae in a control shRNA cell line and SDPR shRNA cells, after transfection of both cell lines with PTRF-mCh and caveolin 1-GFP and FACS sorting of transfected cells. Transfection with PTRF and caveolin 1 caused an increase in the number of caveolae relative to untransfected cells, but there were markedly less caveolae in the SDPR shRNA cells compared to the relevant controls also transfected with PTRF-mCh and caveolin 1-GFP (Figure 3A). Therefore not only does SDPR function during biogenesis of caveolae, but also it is likely to have specific roles in this process beyond regulating PTRF and caveolin 1 expression levels. Additionally, immuno-labeling of cryo-sections of SDPR-GFP-expressing cells and subsequent electron microscopy revealed clear co-localization between caveolin 1 and SDPR in caveolae (Figure 3B). SDPR and caveolin 1 were additionally present in larger tubulo-vesicular structures, as analyzed further below (Figure 3C).

Comparison of the effects of over-expression of PTRF and SDPR offered a way of beginning to further dissect their function within caveolae. Over-expression of PTRF-GFP caused an increase in the number of caveolar membrane invaginations as compared to untransfected cells (Figure 3A), but did not alter the morphology of these invaginations (Figure 3D). In contrast, over-expression of SDPR-GFP did not significantly alter the total number of caveolae, but rather altered their morphology, with many displaying distended and elongated profiles (Figures 3A and 3D). Thus, though both SDPR and PTRF are directly involved in caveolar biogenesis and morphology, they are likely to have differing and specific properties.

SDPR recruits PTRF to plasma membrane caveolae

We expressed PTRF-mCh and caveolin 1-GFP in control and SDPR shRNA cell lines. Reduction in the expression of SDPR caused a visible decrease in the amount of PTRF-mCh present in caveolin 1-GFP puncta in confocal images (Figure 4A). To confirm the loss of PTRF-mCh from the plasma membrane in cells with reduced levels of SDPR, appropriately transfected SDPR shRNA cells and control cells were mechanically lysed and a post-nuclear supernatant subjected to centrifugation at 100,000g in order to pellet membranes. There was much less PTRF-mCh in the membrane fraction (P100) in the SDPR shRNA cells (Figure 4B). In contrast, the amount of SDPR found in the membrane fraction was not altered in PTRF shRNA cells (Figure 4B).

Over-expression of PTRF and SDPR as fusions with GFP or mCh in embryonic fibroblasts from caveolin 1 knockout mice (cav1−/− MEFs) 29 was used to further investigate their function in the absence of caveolin 1. Confocal images showed that, when expressed alone, PTRF has a predominantly cytosolic distribution, whereas SDPR was found associated with the plasma membrane, in patches and tubes (Figure 4C). Co-expression of PTRF and SDPR resulted in translocation of PTRF from the cytosol to the same membrane patches and tubes as SDPR (Figure 4D). PTRF-mCh and SDPR-GFP co-localized in cav1−/− MEFs even at the lowest detectable expression levels (not shown). These data confirm that PTRF associates with protein complexes that also contain SDPR, and that assembly into these complexes is sufficient to recruit PTRF to membranes.

SDPR over-expression generates membrane tubes

Over-expression of SDPR causes accumulation of pronounced tubes in both HeLa and cav1−/− MEF cells, suggesting that SDPR may be able to stablize or generate membrane curvature. Labeling of HeLa cells with fluorescent antibodies against the plasma membrane marker CD59 confirmed that the SDPR-positive tubes are composed of plasma membrane derived membrane, and that these tubes are induced by expression of SDPR as they were not observed in non-transfected cells (Figure 5A). Expression of un-tagged SDPR also resulted in extensive membrane tubulation (Supplementary Figure 5B).

We labeled SDPR-mCh over-expressing HeLa cells with antibodies to caveolin 1 and examined them using the confocal microscope. There was little detectable alteration in the distribution of caveolin 1 in these cells, but 64% (in 20 cells analyzed) of SDPR-positive tubes had a caveolin 1-positive punctum at one end (Figure 5B), and caveolin 1 puncta were also observed along the tube. This is consistent with the observation of SDPR-GFP and caveolin 1 in tubulo-vesicular structures by cryo-electron microscopy (Figure 3C), and suggests that, in cells expressing caveolin 1, SDPR tubes frequently originate from caveolae.

Mutations were made within SDPR to define the minimal region of this protein required to associate with the plasma membrane and generate membrane tubes (Figure 5C). Both the conserved region from amino acids 49-208 that contains putative coiled coils and the

adjacent region characterized by abundant basic amino acid residues (amino acids 219-274) were required for membrane targeting and tubulation. Figure 5D shows schematically SDPR mutants that support this conclusion. Notably, we did not find mutants that were membrane targeted but did not induce tubulation, and replacement of pairs of basic residues in region 219-274 with glutamate was generally sufficient to abolish membrane targeting of over-expressed SDPR (Figures 5C, 5D). Mutations R248E, K237E+K238E, K243E+K244E, K257E+K261E, K272E+K273E, all abolished membrane targeting of full length SDPR. Furthermore, mutants such as SDPR49-290, K272E+K273E that contain the coiled coil region and accumulate in the cytoplasm as puncta could recruit endogenous PTRF to these puncta, thereby confirming that SDPR binds to and recruits PTRF (Supplementary Figure 5A).

SDPR and other caveolar components facilitate STB-induced tubulation of the plasma membrane

Tubular membrane structures have been implicated in the endocytosis of the B-subunit of shiga toxin (STB), and STB induces extensive membrane tubulation in energy-depleted cells 12, 14. As it is unknown whether cytosolic or membrane proteins participate in the formation of these tubes, we asked whether they could be related to the tubes induced by SDPR over-expression. When HeLa cells over-expressing SDPR-GFP were depleted of ATP and labeled with STB there was a high degree of co-localization between STB and SDPR in both tubes and membrane puncta (Figure 6A). Comparing cells expressing the same amount of SDPR-GFP, the number and appearance of SDPR-positive tubes was not altered by the combination of energy poisons and STB (Supplementary Figure 5C). This implies that although STB induces formation of tubes in energy depleted, non-transfected cells 12, when SDPR tubes are already present STB may preferentially enter these tubes.

SDPR tubes originate in caveolae (see Figure 5 above), and in energy-depleted cells SDPR puncta co-localize with STB (Figure 6A). As SDPR puncta co-localize with caveolin 1 (Figures 1B and 1C), we looked for co-localization between caveolin 1 and STB in energy depleted cells. STB in membrane puncta co-localized extensively with caveolin 1-GFP (Figure 6B), and STB-positive membrane tubes frequently had caveolin 1 puncta at one or both ends (Figures 6B and 6C). These data suggest that the tubes induced by SDPR over-expression and the tubes induced by STB labeling of energy-depleted cells both originate in caveolae.

In order to better define the caveolar origin of STB-induced tubes in energy depleted cells we used a combination of time-lapse imaging, TIR imaging, and electron microscopy. The STB-induced tubulation of the plasma membrane was followed in real time with an epifluorescence microscope. Tubes could readily be observed growing from caveolin 1-containing puncta (Figure 7A and Supplementary Movies 1 and 2). TIR, with its very limited depth of illumination, provides a way of ascertaining the plasma membrane proximal end of STB-induced tubes. Analysis of TIR images revealed that 88% of STB-induced tubes had a caveolin 1-positive punctum at that end (n=148 tubes, in 24 separate cells, Figure 7B). These puncta were not always as bright as neighbors that did not define the origin of a STB tube. As caveolae contain a defined amount of caveolin 1 30, this is consistent with the idea that caveolin 1 can also be distributed in puncta elsewhere along the tube (as shown by confocal microscopy in Figure 6C). Indeed, when energy-depeleted, STB-labeled cells were analyzed by immuno-electron microscopy two different types of STB-induced caveolar deformation were observed: caveolin 1-containing caveolae at the plasma-membrane distal end of long tubular invaginations, and membrane tubes emanating from caveolin 1-containing caveolae at the plasma membrane (Figure 7C). STB-induced membrane tubes are at least an order of magnitude less abundant than caveolae (Figure 6B), and accordingly most caveolin 1 antibody labeling was of morphologically normal caveolae (Figure 7C). Put

together, data from a combination of imaging approaches provides strong support for the conclusion that STB-induced tubes in energy depleted cells are derived from caveolae.

In order to assess the role of caveolae in STB uptake without energy depletion we looked for co-localization between caveolin 1 and STB. Although some STB-positive puncta did co-localize, the extent of this co-localization was less than observed after energy depletion (Figure 6B and Supplementary Figure 5D). Tubular intermediates containing STB were observed, albeit markedly less frequently than in energy depleted cells, and these tubes also originated in caveolin 1 puncta (Supplementary Figure 5D). This suggests that in unperturbed HeLa cells uptake in tubular intermediates may account for a minor fraction of total STB internalization, but again the tubes detected are likely to be derived from caveolar membrane invaginations.

As STB-positive tubes were most abundant in energy depleted cells we used that system to assay the functional requirement for SDPR and the other components of caveolae in STB-induced membrane tubulation. ShRNA cell lines, as well as control cells, were energy depleted and labeled with STB so as to induce formation of membrane tubes. The number of tubes over 2 μm in length per cell was counted (Figure 7D). Reduction in SDPR, PTRF or caveolin 1 (Supplementary Figure 5E) expression resulted in a decrease in the amount of tubulation induced by STB (Figure 7D). Cells included in this analysis were selected to have the same amount of bound STB, so reduced tubulation in SDPR shRNA cell lines can not be explained solely by reduction in STB binding. We conclude that the presence of functional caveolae facilitates the formation of STB-induced membrane tubes in cells.

Conclusions

Our data shows that SDPR is present in a complex with PTRF. SDPR promotes recruitment of PTRF to caveolae and has a direct role in formation of caveolar invaginations. Thus formation of caveolae is not solely dependent on oligomerization of caveolin proteins 5, but requires association of further factors. The structure of the multi-molecular assemblies required for characteristic caveolar morphology, with its defined combination of positive and negative membrane curvature, remains to be fully understood. One speculation is that recruitment or modification of PTRF+SDPR-containing complexes is important for changes in caveolar morphology 8, 31, 32.

Over-expressed SDPR can bind to the plasma membrane and induce membrane tubulation, implying that its role within caveolae is directly related to generating curvature. The region of SDPR responsible for membrane tubulation comprises a potentially helical, coiled-coil forming region followed by another conserved domain containing multiple basic amino acids (Figure 5D). There is no obvious sequence similarity between SDPR and known curvature-inducing protein domains, so SDPR may induce curvature by a novel mechanism 33. Further insights will require structural information. SDPR can be recruited to membranes independently from caveolin 1, and binds to phosphatidylserine *in vitro*, making this lipid a good candidate to be the plasma membrane receptor for SDPR 21, 22, 24. PTRF has also been reported to bind to phosphatidylserine 16. Our data implies that this interaction alone is not of sufficiently high affinity to confer plasma membrane localization on PTRF.

STB can enter the cell by multiple mechanisms including clathrin-coated pits, different mechanisms may predominate in different cell types, and it is not clear how the behavior of the toxin in energy depleted cells relates to its uptake under physiological conditions 13, 34, 35. Our data shows that, at least in energy depleted HeLa cells, STB is concentrated in caveolae. Other reports highlight concentration in clathrin-coated pits 13, 35, and we found the co-localization between caveolin 1 and STB to be reduced when cells were not depleted

of energy. STB can induce membrane deformations in liposomes 12, but our data reveals that in cells STB-induced tubes originate from caveolae and that formation of these tubes is less efficient in the absence of caveolar proteins. These results are not incompatible. Caveolae, either because of their lipid composition or the fact that they are pre-curved, clearly represent favored binding sites for STB. The tubulation induced by STB can then be seen as a deformation of caveolae that exploits curvature-inducing caveolar proteins.

Supplementary Material

Refer to Web version on PubMed Central for supplementary material.

Acknowledgments

We would like to thank K. Riento, H. Pelham and S. Munro for comments on the manuscript. C. G. H. is supported by; MRC, Cowi Foundation, Ulla og Mogens Andersens Fond, Oticon Fonden, Julie Von Mullens Fond, Fuhrmann-Fonden, Krista og Viggo Petersen's Fond, Reinholdt W Jorck og Hustrus Fond, Christian og Ottilia Brorsons Rejselegat for Yngre Videnskabsmoend- og Kvinder, Henry Shaw's Legat. N.A.B. is supported by the MRC.

APPENDIX

Materials and Methods

Constructs

cDNA for PTRF from Rattus norvegicus was a generous gift from J. Vinten 17. The cDNA encoding PTRF was PCR amplified with suitable primers forward (GGACTCGAGATGGAGGATGTCACGCTCCATATCGTC) and reverse primer (TGCGAATTCCGTCGCTGTCGCTCTTGTCCACCAG) and was subcloned in the XhoI and EcoRI sites of pEGFP-N1 (Clontech) generating PTRF-EGFP. The EGFP was exchanged with mCherry using BamHI and NotI sites to generate PTRF-mCh.

Human SRBC and SDPR was obtained as cDNA from the I.M.A.G.E. Consortium (clone ID 3882155 and clone ID 4620139 respectively) and PCR amplified with appropriate primers for insertion into the Sal1 and BamHI sites in the pEGFP-N1 vector. Primers used for amplification of SRBC were forward primer CTTGTCGACATGAGGGAGAGTGCGTTGGAGCCGGGGC and reverse primer CACGGATCCGCTCCGGCTACACTCTCCATTTGGAGCAG and for SDPR forward primer CTTGTCGACATGGGAGAGGACGCTGCACAGGCCGAAAAG and reverse primer CTTGGATCCGCTCCGGAGGTCTGGTGCACCTGGAGCACGGCG. mCherry C-terminally tagged version of these constructs were generated by swapping mCherry with EGFP using AgeI and BsrGI. A SDPR C-terminally FLAG tagged construct was also generated in the pEGFP-N1 vector by using the same gene specific forward primers, but by engineering two stop codons following an engineered FLAG - (CTAGGATCCTATTACTTATCGTCGTCATCCTTGTAATCACCTGCCCCGGGTCCGG AGGTCTGGTGCACCTGGAGCACGGCGGGCTGCACG) as the reverse primer. MURC (TrueClone from Origene) accession number XM_294592 was cloned into the EcoRI and SalI sites in pEGFP-N3 (Clontech), resulting in MURC-GFP.

SDPR-CFP containing silent mutations to avoid targeting by SDPR shRNA 2 was produced by site directed mutagenesis of SDPR cDNA inserted in pECFP-N1 vector. Five silent nucleotides substitutions were introduced, from wt nt 5′-961AGTGAGCAG969-3′ to 5′-961TCCGAACAA969-3′.

Generation of SDPR truncation mutants was performed by PCR amplification of SDPR using appropriate primers with SALI and BAMHI restriction sites engineered, the PCR products were then inserted into pEGFP-N1 or pmCherry-N1. Single and double point mutants were generated using site directed mutagenesis.

All PCR generated constructs were sequenced by Geneservice in their entirety to ensure that no PCR generated artefacts were present. Plasmids were transfected into HeLa or MEF cells maintained in DMEM, 10% FCS using Fugene 6 (Roche).

ShRNAs

Stable knock down cell lines were generated using HUSH technology (Origene). A pRS vector expressing an appropriate shRNA 29mer from the U6 promoter was transfected into Hela cells growing in DMEM. One day after transfection the DMEM was supplemented with puromycin at a concentration of 0.7ug/mL. After 14 days in selection media, the cells were reseeded at appropriate dilution to ensure that single clones could be picked. After a further 21 days under selection the isolated clones were assayed for knock down of expression levels of the protein of interest by Western blotting. The constructs targeting PTRF, 5′CACCTTCCACGTCAAGAAGATCCGCGAGG3′ (PTRF shRNA1) and 5′CTGCTGGAGATCACCGAGGAGTCGGACGC3′ (PTRF shRNA2) were purchased from Origene. Controls, (empty pRS vector) and a pRS vector with a non-targetting shRNA cassette 5′TGACCACCCTGACCTACGGCGTGCAGTGC3′ (control shRNA) were also purchased from Origene. We did not observe any difference in the expression levels of the proteins assayed or other characteristics between cell lines generated from the two different control constructs and therefore have used the control shRNA cell line in all figures in this paper. ShRNA constructs targeting human SDPR were generated by ligating two complementary primers and insert them into BamH1 and HINDIII sites in the empty pRS vector. The sequences targeted were 5′CCAGCCTGAAGAAGTGGATAGCCTCAAG3′ (SDRP shRNA 1) and 5′AGTGAGCAGATGCCAAATGACCAGGAAGA3′ (SDRP shRNA 2). Caveolin 1 shRNA HeLa cell lines were produced as described for SDPR. Two separate cell lines targeting 5′TGGAAGGCCAGCTTCACCACCTTCACTGT3′ (Caveolin 1 shRNA1) and 5′AGAGCTTCCTGATTGAGATTCAGTGCATC3′ (Caveolin 1 shRNA2) of the human caveolin 1 mRNA were generated.

Bacterial expression and purification of PTRF and SDPR

pGEX-6P-2 vector was used for N-terminal GST expression of SDPR constructs that were inserted into the EcoRI and NOTI sites. pET28 vector was used for N-terminal 6xHis-tagged expression of PTRF47-268 inserted into the NdeI and EcoRI sites. This construct proved superior in terms of both expression and stability compared to the full length PTRF. Protein expression was carried out using the BL21 strain of *E. coli* grown in LB medium. Expression was induced in bacteria at OD600 = 0.4-0.5 at 18°C with 0.5mM IPTG. The following day the bacteria were spun down, washed in cold PBS, sonicated and spun down for 10 minutes at 3800g. The post nuclear supernatant was spun down at 100000g for 45 minutes. The resulting supernatant was used in a one step batch purification with Glutathionine Sepharose or Ni-NTA agarose as appropriate.

Immunoprecipitations

Hela cells were transfected with constructs of interest 36 hours prior to harvest. Immunoprecipitations were carried out using the μMacs Epitope Tag Protein Isolation Kit (Miltenyi Biotec). Cells were lysed directly into the provided lysis buffer (which contains 1% Triton X-100), supplemented with protease inhibitors and 1% n-β-Octylglycoside (OG). Solubilization was carried out for 2 hours on a roller at 4°C. Non-solubilized material was removed by ultracentrifugation at 100000rpm in a Beckman TL120.2 rotor. Magnetic beads

conjugated to anti-GFP antibodies were added to the remaining sample and incubated at 4°C for 1 hour. Samples were applied to μMACS magnetic columns, 0.2% OG was added to the provided washing buffer. Protein complexes were eluted by pH shift (0.1M Triethyl Amine, 0.1% Triton X100, pH11).

Antibodies

Peptides against amino acids 9-23 and 312-325 of human SDPR were used to immunise the same rabbit. Resultant antiserum was purified using immobilised peptides. This was carried out by Eurogentec. Sources for other antibodies were as follows: mouse monoclonal anti-c-Myc 9E10 (Sigma), rabbit polyclonal anti-PTRF (Abcam), mouse monoclonal anti-PTRF (Abnova), polyclonal rabbit anti-GFP (Abcam), polyclonal rabbit anti-FLAG (Sigma), polyclonal rabbit anti-caveolin 1 and monoclonal mouse anti-caveolin 1 (both BD Biosciences), polyclonal anti-dsRed (recognizes mCherry, Clontech). HRP-conjugated secondaries were from DAKO and the ECL western Blotting detection Kit was from GE Healthcare. Protein A conjugated to 10 and 15 nm colloidal gold was purchased from the Department of Cell Biology, University of Utrecht.

Light Microscopy

TIR images were acquired with an Olympus TIR illumination system, via a 100x 1.45NA objective. Confocal images were acquired with a Zeiss LSM510. Standard FITC and Rhodamine filter sets were used for imaging GFP and mCh fluorescence.

Electron microscopy

For both resin-embedded and cryo-electron microscopy transfected cells were sorted away from untransfected cells by FACS. They were then re-plated and allowed to grow overnight to regain normal cell morphology. For microscopy of resin-embedded sections cells grown in Petri dishes were briefly washed twice with PBS and then fixed in 2% paraformaldehyde (PFA) and 2.5% glutaraldehyde in 0.1M Na Cacodylate, pH 7.2. They were scraped off, and centrifuged in a horizontal rotor and the pellets were embedded in 2% agar and cut into 1mm3 blocks and placed in fresh fixative. Cells were fixed at room temperature for an hour and then stored at 4°C. Samples were washed thoroughly in 0.1M Na Cacodylate buffer and post fixed in 1% OsO4 (in 0.1M Na Cacodylate) for 1 hour and then washed with distilled water. Samples were then en bloc stained with 2% uranyl acetate in 30% ethanol followed by dehydration in a graded ethanol series followed 1,2, epoxy propane (propylene oxide) and then infiltrated and embedded in CY212 resin (Agar Scientific).

For pre-embedding immunogold electron microscopy cells were washed with PBS and fixed in 4% paraformaldehyde, 0.1M sodium cacodylate buffer (pH 7.4) for 2 hours at room temperature. After 3 × 10 min washes in cacodylate buffer, the cells were pelleted in eppendorf tubes (4000 rpm for 8 min - this applied to each subsequent step when changing buffers), washed twice in 0.05M Tris /HCl/0.15M NaCl, pH 7.4 (TBS). Cells were then permeabilised in TBS with 0.05% Saponin, also containing 3% BSA, 0.02M glycine, for 30 mins. Note that saponin was added to all subsequent TBS incubation and wash steps. The cells were then incubated in rabbit anti caveolin antisera (1:20 dil) for 2 hrs at room temperature, washed in TBS and incubated with goat anti rabbit IgG conjugated to 10nm gold (BB International) for 1 hour. Cells were then washed and finally fixed in 2% glutaraldehyde in cacodylate buffer, post fixed and embedded in CY212.

Ultrathin 50 - 70 nm sections were cut on a Reichert Ultracut E microtome and collected on uncoated 200 mesh grids. Sections were post stained with saturated uranyl acetate followed by Reynolds lead citrate. Images were acquired using a Philips EM208 microscope at an operating voltage of 80 kV, using a CCD camera.

Immunogold cryo-electron microscopy was carried out as follows. Hela cells expressing GFP-tagged SDPR were washed with PBS, fixed with 4% paraformaldehyde / 0.1% glutaraldehyde in 0.1M sodium cacodylate buffer (pH 7.2) and pelleted in an eppendorf tube (13 000rpm for 5 min). The fixative was aspirated and the cell pellet was re-suspended in warm 10% gelatin in PBS. The cells were then pelleted (13 000rpm for 5 min) and the gelatin-enrobed cells were set on ice, trimmed into $1mm^3$ blocks and infused with 1.7M sucrose / 15% poly vinyl pyrolidone for 24h at 4°C. The blocks were subsequently mounted on cryostubs and snap-frozen in liquid nitrogen. Frozen ultrathin sections were cut using a diamond knife in an ultramicrotome with a cryochamber attachment (Leica, Milton Keynes, UK) at −120°C, collected from the knife-edge with 50:50 2% methyl cellulose: 2.3 M sucrose (Liou et al. 1996) and mounted on formvar-carbon coated EM grids.

Sequential immunolabeling of caveolin and EGFP was performed using the protein A-gold technique at room temperature (Slot et al. 1991). The sections were contrasted by embedding in 1.8% methyl cellulose / 0.3% uranyl acetate and air-dried prior to observation in a Philips CM100 transmission electron microscope at an operating voltage of 80kV.

Cell labeling and indirect immunofluorescence

STB-Cy3 was a gift from F. Barr 36. STB-Cy3 was used at a final concentration of $0.5\mu g.ml^{-1}$. ATP depletion was carried out by incubating cells with 10mM NaN_3 and 10mM 2-deoxyglucose in PBS^{++}, exactly as described 12. For indirect immunofluorescence cells were fixed in 4% formaldehyde pre-warmed to 37°C, as we found this gave improved preservation of membrane tubes. Antibody incubations were performed in PBS with 10% FCS, 0.2% saponin.

References

1. Mayor S, Pagano RE. Pathways of clathrin-independent endocytosis. Nat Rev Mol Cell Biol. 2007; 8:603–612. [PubMed: 17609668]
2. Kirchhausen T. Three ways to make a vesicle. Nat Rev Mol Cell Biol. 2000; 1:187–198. [PubMed: 11252894]
3. Stagg SM, LaPointe P, Balch WE. Structural design of cage and coat scaffolds that direct membrane traffic. Curr Opin Struct Biol. 2007; 17:221–228. [PubMed: 17395454]
4. Lajoie P, Nabi IR. Regulation of raft-dependent endocytosis. J Cell Mol Med. 2007; 11:644–653. [PubMed: 17760830]
5. Bauer M, Pelkmans L. A new paradigm for membrane-organizing and - shaping scaffolds. FEBS Lett. 2006; 580:5559–5564. [PubMed: 16996501]
6. Le Lay S, Kurzchalia TV. Getting rid of caveolins: Phenotypes of caveolin-deficient animals. Biochim Biophys Acta. 2005
7. Parton RG, Richards AA. Lipid rafts and caveolae as portals for endocytosis: new insights and common mechanisms. Traffic. 2003; 4:724–738. [PubMed: 14617356]
8. Stan RV. Structure and function of endothelial caveolae. Microsc Res Tech. 2002; 57:350–364. [PubMed: 12112442]
9. Pelkmans L, Burli T, Zerial M, Helenius A. Caveolin-stabilized membrane domains as multifunctional transport and sorting devices in endocytic membrane traffic. Cell. 2004; 118:767–780. [PubMed: 15369675]
10. Kirkham M, et al. Ultrastructural identification of uncoated caveolin-independent early endocytic vehicles. J Cell Biol. 2005; 168:465–476. [PubMed: 15668297]
11. Kumari S, Mayor S. ARF1 is directly involved in dynamin-independent endocytosis. Nat Cell Biol. 2008; 10:30–41. [PubMed: 18084285]
12. Romer W, et al. Shiga toxin induces tubular membrane invaginations for its uptake into cells. Nature. 2007; 450:670–675. [PubMed: 18046403]

13. Lauvrak SU, et al. Shiga toxin regulates its entry in a Syk-dependent manner. Mol Biol Cell. 2006; 17:1096–1109. [PubMed: 16371508]
14. Sandvig K, et al. Pathways followed by protein toxins into cells. Int J Med Microbiol. 2004; 293:483–490. [PubMed: 15149022]
15. Liu L, Pilch PF. A critical role of cavin (polymerase I and transcript release factor) in caveolae formation and organization. J Biol Chem. 2008; 283:4314–4322. [PubMed: 18056712]
16. Hill MM, et al. PTRF-Cavin, a conserved cytoplasmic protein required for caveola formation and function. Cell. 2008; 132:113–124. [PubMed: 18191225]
17. Vinten J, Johnsen AH, Roepstorff P, Harpoth J, Tranum-Jensen J. Identification of a major protein on the cytosolic face of caveolae. Biochim Biophys Acta. 2005; 1717:34–40. [PubMed: 16236245]
18. Aboulaich N, Vainonen JP, Stralfors P, Vener AV. Vectorial proteomics reveal targeting, phosphorylation and specific fragmentation of polymerase I and transcript release factor (PTRF) at the surface of caveolae in human adipocytes. Biochem J. 2004; 383:237–248. [PubMed: 15242332]
19. Vinten J, et al. A 60-kDa protein abundant in adipocyte caveolae. Cell Tissue Res. 2001; 305:99–106. [PubMed: 11512676]
20. Liu L, et al. Deletion of Cavin/PTRF causes global loss of caveolae, dyslipidemia, and glucose intolerance. Cell Metab. 2008; 8:310–317. [PubMed: 18840361]
21. Gustincich S, Schneider C. Serum deprivation response gene is induced by serum starvation but not by contact inhibition. Cell Growth Differ. 1993; 4:753–760. [PubMed: 8241023]
22. Gustincich S, et al. The human serum deprivation response gene (SDPR) maps to 2q32-q33 and codes for a phosphatidylserine-binding protein. Genomics. 1999; 57:120–129. [PubMed: 10191091]
23. Mineo C, Ying YS, Chapline C, Jaken S, Anderson RG. Targeting of protein kinase Calpha to caveolae. J Cell Biol. 1998; 141:601–610. [PubMed: 9566962]
24. Burgener R, Wolf M, Ganz T, Baggiolini M. Purification and characterization of a major phosphatidylserine-binding phosphoprotein from human platelets. Biochem J. 1990; 269:729–734. [PubMed: 2390065]
25. Izumi Y, et al. A protein kinase Cdelta-binding protein SRBC whose expression is induced by serum starvation. J Biol Chem. 1997; 272:7381–7389. [PubMed: 9054438]
26. Ogata T, et al. MURC, a muscle-restricted coiled-coil protein that modulates the Rho/ROCK pathway, induces cardiac dysfunction and conduction disturbance. Mol Cell Biol. 2008; 28:3424–3436. [PubMed: 18332105]
27. Tagawa M, et al. MURC, a muscle-restricted coiled-coil protein, is involved in the regulation of skeletal myogenesis. Am J Physiol Cell Physiol. 2008; 295:C490–498. [PubMed: 18508909]
28. Merrifield CJ, Feldman ME, Wan L, Almers W. Imaging actin and dynamin recruitment during invagination of single clathrin-coated pits. Nat Cell Biol. 2002; 4:691–698. [PubMed: 12198492]
29. Razani B, et al. Caveolin-1 null mice are viable but show evidence of hyperproliferative and vascular abnormalities. J Biol Chem. 2001; 276:38121–38138. [PubMed: 11457855]
30. Pelkmans L, Zerial M. Kinase-regulated quantal assemblies and kiss-and-run recycling of caveolae. Nature. 2005; 436:128–133. [PubMed: 16001074]
31. Kirkham M, et al. Evolutionary analysis and molecular dissection of caveola biogenesis. J Cell Sci. 2008; 121:2075–2086. [PubMed: 18505796]
32. Rothberg KG, et al. Caveolin, a protein component of caveolae membrane coats. Cell. 1992; 68:673–682. [PubMed: 1739974]
33. Zimmerberg J, Kozlov MM. How proteins produce cellular membrane curvature. Nat Rev Mol Cell Biol. 2006; 7:9–19. [PubMed: 16365634]
34. Nichols BJ, et al. Rapid cycling of lipid raft markers between the cell surface and Golgi complex. J Cell Biol. 2001; 153:529–541. [PubMed: 11331304]
35. Sandvig K, van Deurs B. Entry of ricin and Shiga toxin into cells: molecular mechanisms and medical perspectives. Embo J. 2000; 19:5943–5950. [PubMed: 11080141]
36. Fuchs E, et al. Specific Rab GTPase-activating proteins define the Shiga toxin and epidermal growth factor uptake pathways. J Cell Biol. 2007; 177:1133–1143. [PubMed: 17562788]

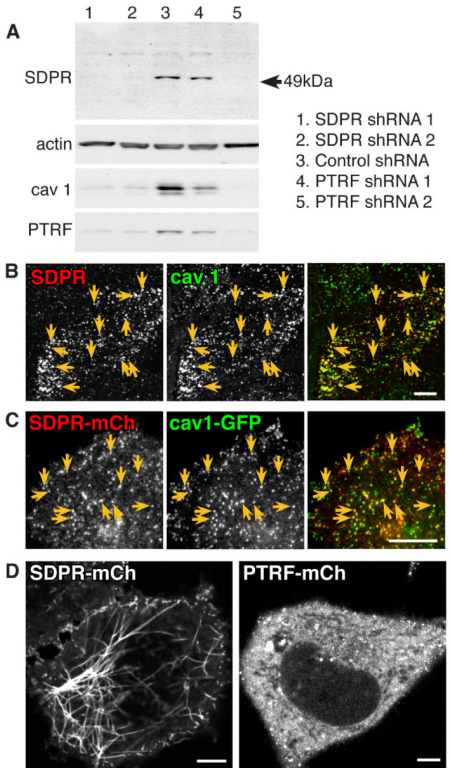

Figure 1. SDPR is a caveolar protein, but forms tubes at high expression levels

A. Western blots showing expression levels of SDPR, actin, caveolin 1 and PTRF in HeLa cell lines stably transfected with plasmids expressing shRNAs as shown. Arrow indicates position of 49kDa size marker (ovalbumin, not visible). Complete scans of the blots are shown in Supplementary Figure 6. **B**. Confocal image of a HeLa cell labeled using indirect immunofluorescence with monoclonal anti-caveolin 1 and polyclonal anti-SDPR. Yellow arrows highlight co-localization, bar 10μm. **C**. TIR image of caveolin 1-GFP and SDPR-mCh expressed in a HeLa cell. Yellow arrows highlight co-localization. Bar 10μm. **D**. Over-expression of SDPR-mCh at approximately 10x endogenous protein levels results in formation of extensive tubes. PTRF over-expressed at the same levels has a predominantly cytosolic distribution. Confocal images of live HeLa cells. Bars 10μm.

Europe PMC Funders Author Manuscripts

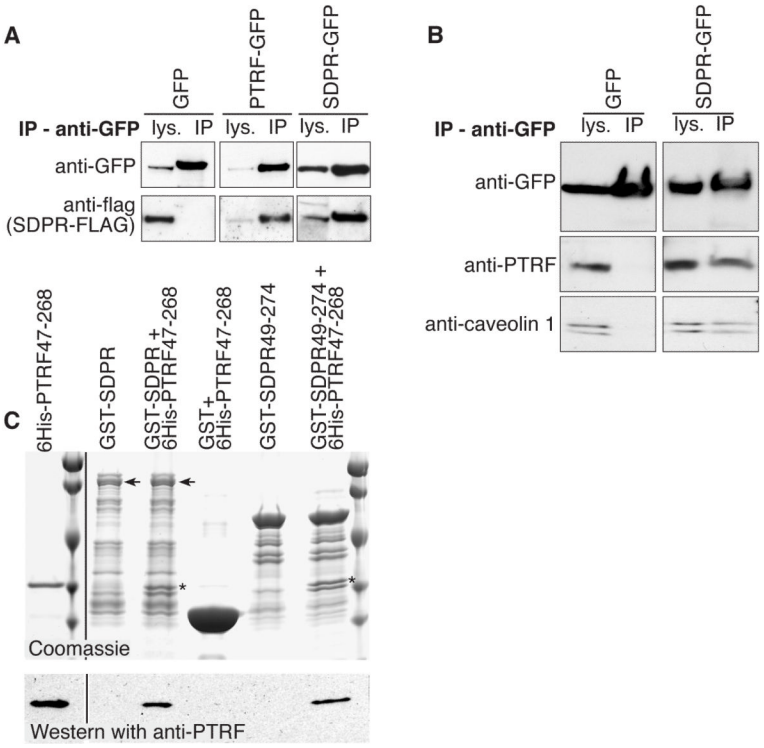

Figure 2. SDPR is present in protein complexes with PTRF and caveolin 1 and can bind directly to PTRF *in vitro*

A. Immunoprecipitation of PTRF-GFP and SDPR-GFP expressed in HeLa cells with anti-GFP antibodies results in co-precipitation of SDPR-FLAG as shown. Immunoprecipitation of GFP did not result in co-precipitation. **B**. Immunoprecipitation of SDPR-GFP expressed in HeLa cells with anti-GFP antibodies results in specific co-precipitation of endogenous PTRF and caveolin 1 detected by Western blotting as shown. **C**. After purification on Ni-Agarose 6His-PTRF47-268 (left hand lane) was applied to GST-SDPR, GST-SDPR49-274, or GST immobilized on glutathione sepharose as indicated. Eluted proteins were analyzed by SDS-PAGE and Coomassie staining or Western blotting. The band marked with an arrow is intact GST-SDPR, other bands in the GST-SDPR lane are predominantly degradation products as determined by Western blotting with SDPR antibodies (not shown). The * highlights 6His-PTRF47-268 specifically bound to SDPR and SDPR49-274. Complete scans of all blots and gels are shown in Supplementary Figure 6.

Europe PMC Funders Author Manuscripts

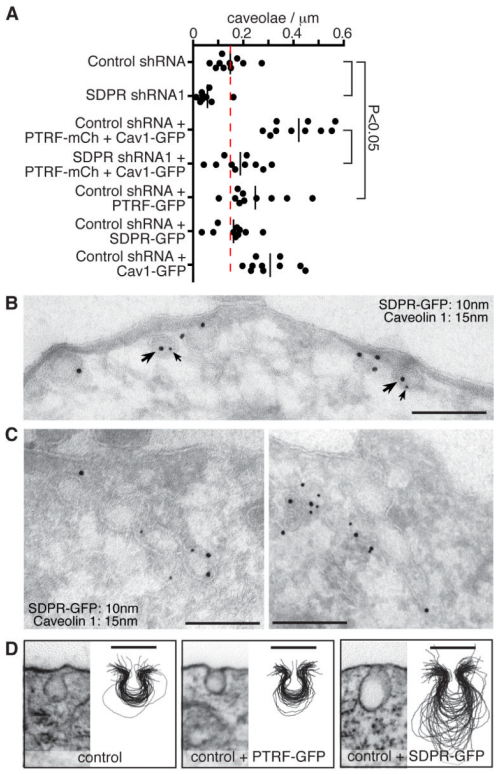

Figure 3. SDPR is required for formation of caveolar membrane invaginations, and induces formation of elongated caveolae when over-expressed

A. The frequency of caveolae in HeLa cell lines stably transfected with different shRNAs, and transiently transfected with plasmids as shown. Transiently transfected cells were selected using FACS. For each cell line electron micrographs generating complete sections through 10 cells were analyzed (See Supplementary Figure 5). Black bars are the mean for each sample, dashed red line shows the mean for control cells. P values were calculated with an unpaired *t*-test. **B**. Immunolabeling of cryo-sections of SDPR-GFP expressing cells with antibodies against caveolin 1 (15nm gold, large arrows) and GFP (10nm gold, small arrows). Bar 200nm. **C.** Immunolabeling of cryo-sections of SDPR-GFP expressing cells with antibodies against caveolin 1, as in B. Examples of extended caveolae and tubulo-vesicular structures containing SDPR and caveolin 1 are shown. Bar 200nm. **D**. Morphology of caveolae in cells over-expressing PTRF or SDPR. Electron micrographs of typical caveolae from each cell line are shown, together with manually superimposed caveolar membrane profiles from 50 caveolae (see Supplementary Figure 5). Bars are 100nm.

Europe PMC Funders Author Manuscripts

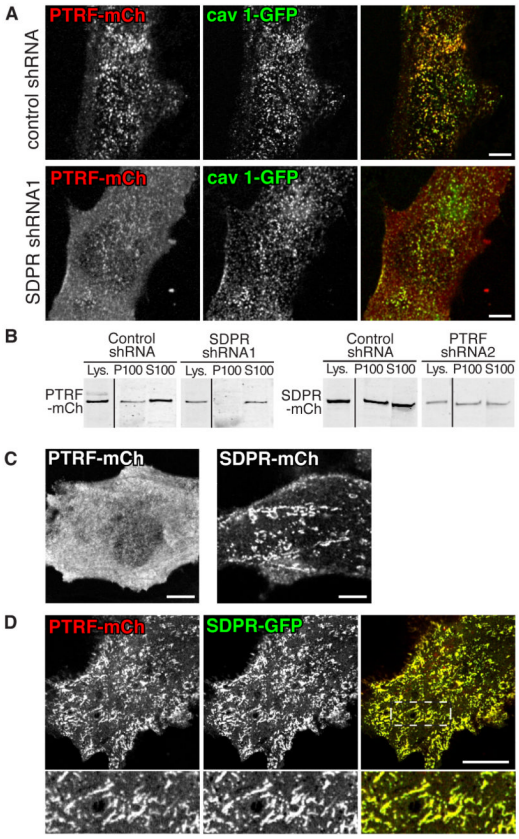

Figure 4. SDPR recruits PTRF to caveolae and to the plasma membrane

A. Recruitment of PTRF-mCh to caveolin 1-GFP puncta in cells stably transfected with control and SDPR shRNAs, visualized by confocal microscopy. Cells expressing the same total amount of PTRF-mCh and caveolin 1-GFP are shown. Bars 10μm. **B**. Fractionation of post-nuclear supernatants from control, SDPR and PTRF shRNA cell lines transfected with PTRF-mCh and caveolin 1-GFP (left hand Western blot) or SDPR-mCh and caveolin 1-GFP (right hand Western blot). Lys. = cell lysate prepared by solubilization of the post-nuclear supernatant in SDS-PAGE sample buffer. P100 = membrane pellet at 100,000g, S100 = supernatant at 100,000g. Blots were probed with anti-mCh antibodies, fluorescent secondary antibodies, and analyzed using a Licor Odyssey fluorescence scanner for linear detection. Complete scans of the blots are shown in Supplementary Figure 6. **C.** Confocal images showing distribution of PTRF-mCh and SDPR-mCh expressed individually at similar levels in cav1−/− MEFs. Bars 10μm. **D**. Co-expression of PTRF-mCh and SDPR-GFP in cav1−/− MEFs results in recruitment of PTRF-mCh to SDPR-GFP membrane patches and tubes. Bar 10μm. The lower panels are a magnified view of the region delineated by a dashed line.

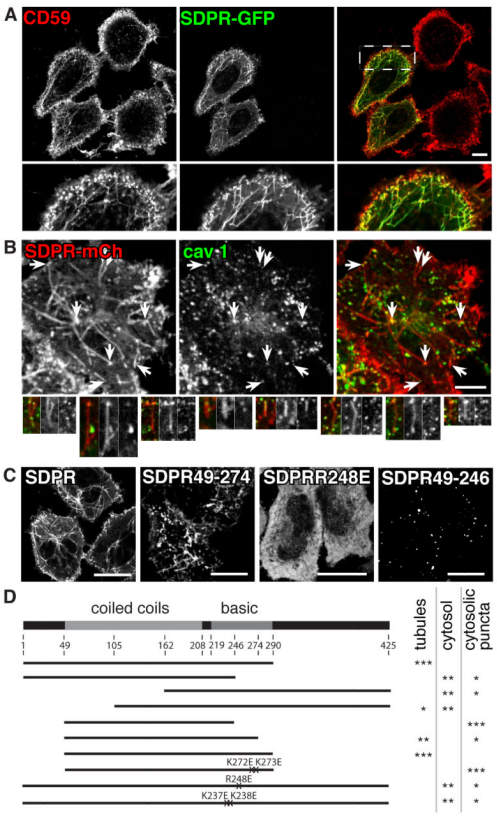

Figure 5. SDPR over-expression induces membrane tubes derived from caveolae

A. Labeling of HeLa cells, two of which are over-expressing SDPR-GFP, with fluorescent antibodies against the GPI-linked protein CD59. Live cells were labeled for 20min prior to imaging. The lower panels show a magnified view of the region denoted by the dashed line. Confocal images. Bar 20μm. **B.** Localization of caveolin 1 to the ends of SDPR-mCh positive membrane tubes. Caveolin 1 was detected with polyclonal antibodies using indirect immunofluorescence. Bar 10μm. The lower panels show further examples of SDPR-induced membrane tubes with caveolin 1 puncta at one end. All images are confocal. **C**. Different distribution of over-expressed SDPR mutants. Different GFP-tagged mutants of SDPR as indicated were over-expressed at similar levels in live HeLa cells and imaged by confocal microscopy. Bar 20μm. **D**. Mapping of the region of SDPR required for membrane targeting and tubulation. The diagram indicates a selected subset of all constructs analyzed, with a score representing their sub-cellular distribution based on up to 3 stars. Only over-expressing cells were analyzed - some mutants that are not membrane targeted when over-expressed are still found in caveolae when expressed at low levels, presumably because of binding to endogenous SDPR or another caveolar component. Construct 105-425 was occasionally observed in the nucleus as well as the cytosol.

Europe PMC Funders Author Manuscripts

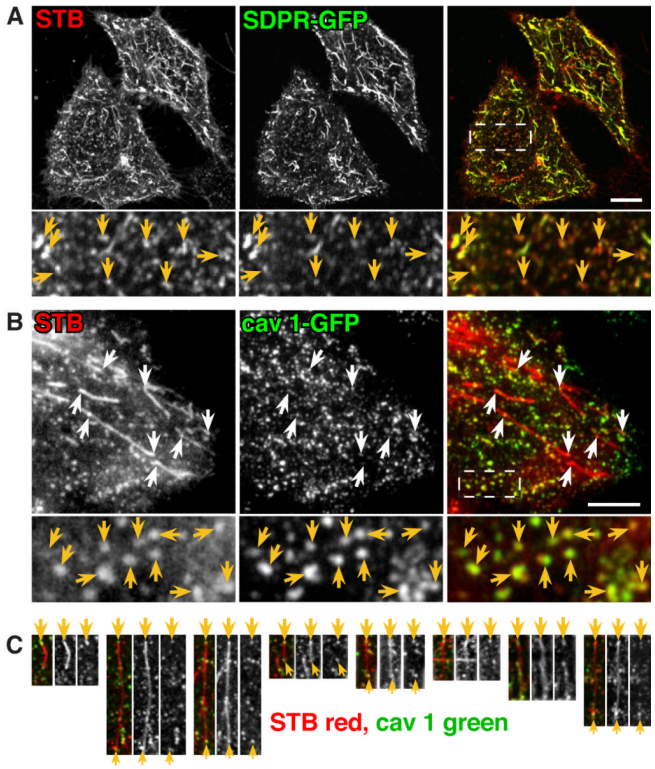

Figure 6. Membrane tubes induced by shiga toxin B-subunit co-localize with SDPR and caveolin 1

A. Co-localization between over-expressed SDPR-GFP and STB-Cy3 in energy depleted HeLa cells. Confocal image of live cells. Bar is 20μm. The lower panels show a magnified view of the region delineated by the dashed line. Yellow arrows highlight extensive co-localization in membrane puncta. **B**. Localization of caveolin 1-GFP to the ends of STB-induced tubes and co-localization between caveolin 1 and STB puncta, in unfixed energy depleted cells. Confocal image. Bar 10μm. White arrows indicate examples of localization of caveolin 1 to the end of STB-positive tubes. The lower panels show a magnified view of the region delineated by the dashed line. Yellow arrows highlight co-localization in membrane puncta. **C.** Further examples of localization of caveolin 1 to the ends of STB tubes are shown. Tubes are lined up using caveolin 1 puncta at one end of the tube, indicated with the large arrows. Some tubes also have caveolin 1 puncta at the other end of the tube, indicated using small arrows.

Europe PMC Funders Author Manuscripts

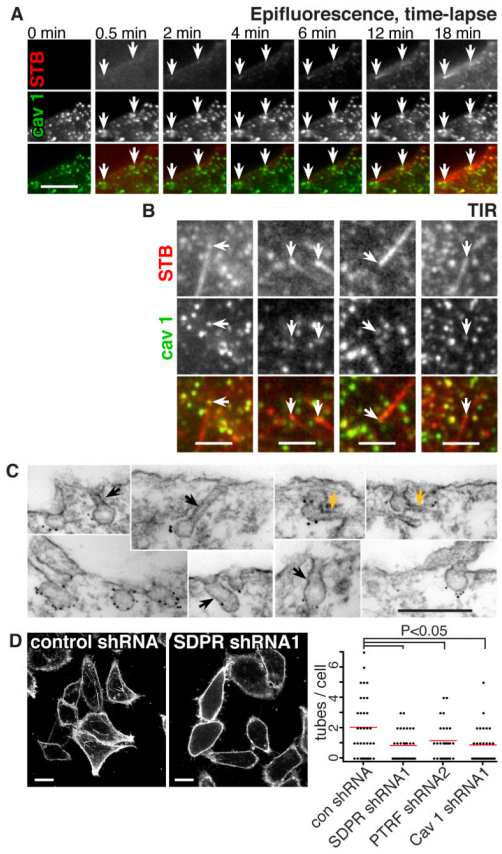

Figure 7. STB-induced membrane tubes grow from caveolae, and their formation is facilitated by caveolar proteins

A. Time-lapse epifluorescence images of addition of STB to an energy-depleted HeLa cell expressing caveolin 1-GFP. STB was added at time zero. Arrows indicate STB-induced tubules growing out from caveolin 1-positive puncta. See also Supplementary Movies 1 and 2. Bar is 2μm. **B.** Montage of TIR images of STB-labeled, energy-depleted, unfixed HeLa cells expressing caveolin 1-GFP. Arrows indicate caveolin 1 puncta at the membrane-proximal end of STB-induced tubes. Each series of panels is from a different cell. Bar is 2μm. **C.** Pre-embedding immuno-electron microscopy of energy depleted cells after treatement with STB. Labeling is with polyclonal anti-caveolin 1 antibodies and 10nm gold-conjugated secondary antibodies. Black arrows indicate caveolae with STB-induced membrane tubes connecting them to the plasma membrane, and yellow arrows indicate caveolae at the plasma membrane with STB-induced membrane tubes emanating from them. Normal caveolae are also shown for comparison. Bar is 200nm. **D.** Effect of reduced SDPR, PTRF and caveolin 1 expression on STB-induced membrane tubulation in energy depleted cells. Images are of live HeLa cell lines stably transfected with the shRNAs shown. Quantification is of the number of STB-positive membrane tubes in the different cell lines shown. The red bars are the mean for each sample. P values were calculated with an unpaired *t*-test.